ENVIRONMENTALLY-ASSISTED FATIGUE CRACK GROWTH IN PRESTRESSING STEEL WIRES

J. TORIBIO, J. C. MATOS, B. GONZÁLEZ, J. ESCUADRA

University of Salamanca, Campus Viriato, Zamora, Spain

This paper presents the evolution of the surface crack front in prestressing reinforced concrete steel wires subjected to fatigue in air and to corrosion-fatigue in $Ca(OH)_2$+NaCl. To this end, a numerical modelling was made on the basis of a discretization of the crack front (with elliptical shape), considering that the crack advance at each point is perpendicular to such a front according to a Paris-Erdogan law, and using a three-parameter solution for stress intensity factor (SIF). Each analyzed case (a particular initial crack geometry) was characterized by the evolution of the semielliptical crack aspect ratio (relation between the semiaxes of the ellipse) with the relative crack depth and by the variation of the maximum dimensionless SIF at the crack front.

Keywords: *numerical modelling, fatigue crack propagation, prestressing steel bars, $Ca(OH)_2$+NaCl corrosion-fatigue.*

The fatigue behaviour of cold drawn eutectoid steel, frequently used as reinforcement in prestressed concrete, had received attention in the past, both in air [1] and in aggressive environments [2–6]. NaCl corrosion-fatigue affects the fatigue performance of high strength steel by increasing the crack growth rate in relation to its value in inert environment [3, 4], this effect being even higher if the environment is constituted by $Ca(OH)_2$+NaCl [5].

When cylindrical rods (bars, wires, shafts…) are used, transverse cracking by fatigue usually takes place in the form of surface cracks with a semielliptical shape [7]. Growth of surface cracks in round bars due to fatigue can be modelled using different criteria, e.g., prediction of the 90° intersecting angle of the crack with the surface or the iso-K criterion along the crack front [8]. Another criterion is based on the crack growth according to the Paris-Erdogan law [9], considering the crack advance perpendicular to the crack front, assuming elliptic geometry for the growing crack [10, 11] or avoiding the shape hypothesis, i.e., allowing the crack to grow with any shape [12].

Material. This paper studies the corrosion-fatigue crack propagation in prestressing steel wires (chemical composition: 0.82% C; 0.60% Mn; 0.18% Si; 0.010% P and 0.024% S) of 7 mm diameter. Mechanical properties of the steel were obtained by Singh and Sánchez–Gálvez [5] as follows: Young's modulus E = 204.4 GPa, yield strength σ_Y = 1430 MPa, ultimate tensile strength (UTS) σ_R = 1670 MPa and fracture toughness K_{IC} = 119 MPam$^{1/2}$. Fatigue tests were performed [5] under 1 Hz sinusoidal wave and R-ratio equal to 0.5 in both air and aggressive environment consisting of 1 g/l $Ca(OH)_2$ + 1 g/l NaCl solution at free corrosion potential, and results were fitted to a Paris-Erdogan law [9] in the form:

$$\frac{da}{dN} = C\Delta K^{\mathrm{m}} \tag{1}$$

obtaining the coefficients of the Paris law for prestressing steel in both environments.

Corresponding author: J. TORIBIO, e-mail: toribio@usal.es

With regard to Paris exponent m, experimental results were $m = 2.27$ for fatigue crack propagation in air and $m = 0.70$ in the case of $Ca(OH)_2$ + NaCl corrosion-fatigue, where a clear decrease in the m-exponent was observed in corrosion-fatigue in spite of the elevation of the curve via an increase of the C coefficient, from $1.78 \cdot 10^{-11}$ for fatigue crack propagation in air to $2.04 \cdot 10^{-8}$ in the case of $Ca(OH)_2$+NaCl corrosion-fatigue (with the corresponding units for ΔK in $MPam^{1/2}$ and da/dN in m/cycle).

Numerical modelling. To study how a crack propagates in the cross section of a round bar under tension cyclic loading, a computer program in Java language was developed to determine the geometrical evolution of the crack front. The basic hypothesis of the modelling consists in assuming that the crack front can been modelled as an ellipse with a centre on the bar surface [7] and the fatigue propagation takes place in the direction perpendicular to this crack front, following a Paris-Erdogan law [9].

Every elliptical arc of the crack was divided in z segments with exactly the same length using the Simpson method to discretize the front. The point on the cylinder surface is not taken into account, since it presents difficulties regarding the computation of the stress intensity factor (SIF) K because there is a plane stress state at the crack edge. After that, every single point was shifted according to Paris-Erdogan law perpendicular to the front, to keep constant the maximum crack depth increment, $\Delta a(\max) \equiv \max \Delta a_i$. The advance of every front point, Δa_i, can be obtained from the maximum crack increment and the ratio of the dimensionless SIF

$$Y = K \big/ \sigma\sqrt{\pi a} \,, \tag{2}$$

(where σ is the remote stress applied far from the crack and a is the crack depth) as follows:

$$\Delta a_i = \Delta a(\max)\left[\frac{Y_i}{Y(\max)}\right]^m . \tag{3}$$

The newly obtained points, fitted by the least squares method, generate a new ellipse with which the process of crack advance is repeated iteratively until the desired crack depth is reached (the maximum crack advance was up to 80% of the bar diameter). Due to the existing symmetry, only half of the problem was used for the computations.

The number of cycles necessary for fatigue crack propagation, from the initial crack depth a_i to the final crack depth a_f, can be obtained by introducing the equation to calculate the SIF range,

$$\Delta K = Y \Delta\sigma\sqrt{\pi a} \tag{4}$$

in the Paris-Erdogan law, obtaining the expression,

$$N = \frac{1}{C\Delta\sigma^m \pi^{m/2}} \int_{a_i}^{a_f} \frac{da}{Y^m a^{m/2}} = \frac{1}{C\Delta\sigma^m \pi^{m/2} D^{(m-2)/2}} \int_{a_i}^{a_f} \frac{da/D}{Y^m \left(a/D\right)^{m/2}} . \tag{5}$$

n, the dimensionless number of cycles, is given by,

$$n = \int_{a_i}^{a_f} \frac{da/D}{Y^m \left(a/D\right)^{m/2}} , \tag{6}$$

where the SIF is calculated at the central point in the crack x/h=0 (and thus the dimensionless SIF becomes dependent on two parameters) and the integral is incrementally computed by applying the trapezoidal rule for the successive crack advances.

Dimensionless SIF. The dimensionless SIF used in the computations performed in this paper is that proposed by Shin and Cai [13] obtained by the finite element method

together with a virtual crack extension technique, which depends on the crack geometry a/b (aspect ratio, relation between the semiaxes of the ellipse), the relative crack depth a/D and the relative position of the point considered on its front x/h (Fig. 1).

The analytical fitting on the basis of the finite element results provides a three-parameter expression of the dimensionless SIF Y as follows,

$$Y = \sum_{i=0}^{2} \sum_{j=0}^{7} \sum_{k=0}^{2} M_{ijk} \left(\frac{a}{b}\right)^i \left(\frac{a}{D}\right)^j \left(\frac{x}{h}\right)^k , \quad (7)$$

where the coefficients M_{ijk} used in the present paper are those calculated by Shin and Cai [13] for the particular case of tension loading with free ends (see Table).

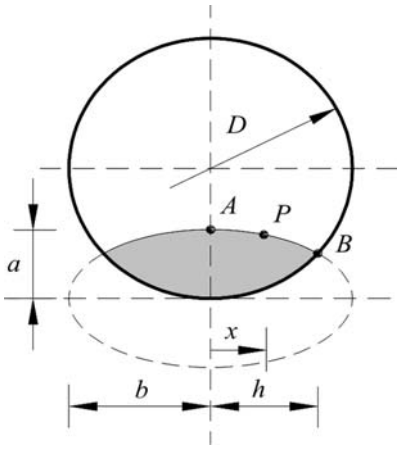

Fig. 1. Elliptical crack model used by Shin and Cai.

SIF coefficients M_{ijk} for tension with free ends proposed by Shin and Cai [13]

i	j	$k = 0$	$k = 1$	$k = 2$
0	0	0.220	0.123	–0.409
0	1	28.513	0.511	–9.764
0	2	–354.782	–2.034	128.817
0	3	2178.632	–19.569	–727.078
0	4	–7140.202	144.435	2201.067
0	5	12957.447	–359.284	–3732.813
0	6	–12227.977	393.518	3343.521
0	7	4721.868	–159.206	–1240.214
1	0	–0.326	0.065	1.011
1	1	–3.780	–6.878	–3.946
1	2	79.489	47.747	41.099
1	3	–571.094	–119.954	–316.682
1	4	1976.255	14.769	1284.860
1	5	–3583.421	423.169	–2563.292
1	6	3256.770	–661.610	2455.158
1	7	–1163.158	306.176	–880.302
2	0	0.266	0.118	–1.584
2	1	–9.118	–3.515	45.562
2	2	85.381	75.016	–552.891
2	3	–465.013	–587.594	3322.477
2	4	1475.911	2197.404	–10812.317
2	5	–2794.532	–4264.810	19328.127
2	6	2878.868	4138.287	–17829.715
2	7	–1261.348	–1588.135	6638.698

The choice of the most adequate K-value in a round bar (to be used in this research) was made on the basis of the critical review in [14] (Fig. 2). The K-solution depends on the number of parameters involved in the analysis, namely: (i) when only one parameter such as the relative crack depth (a/D) is required, the pioneering solution by Valiente is very adequate for straight-fronted (or very slightly-curved) edge-cracks; (ii) when two parameters such as the relative crack depth (a/D) and the crack aspect ratio

(*a*/*b*) are needed, the solution by Astiz is the most adequate for obtaining the SIF at the crack centre (it exhibits the best performance of all of them!), whereas Carpinteri provides good solutions at the crack surface; (iii) when three parameters such as the relative crack depth (*a*/*D*), the crack aspect ratio (*a*/*b*) and the position at the crack front (*x*/*h*) are required (as in the case of the present research work on corrosion-fatigue of high-strength prestressing steels), the solutions by Shin and Cai are recommended (although they do not work as well as that of Astiz), and in addition they are the only which distinguish between free ends and constrained ends in the analysis.

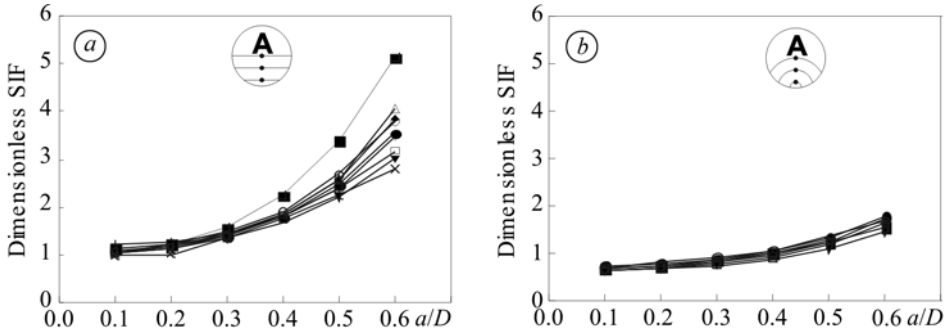

Fig. 2. Critical review [14] of SIF solutions at the crack centre (point *A*): straight crack front, $a/b = 0$ (*a*), and circular crack front, $a/b = 1$ (*b*): × – Valiente 1 [15]; + – Valiente 2 [15]; ● – Astiz [16]; ○ – Carpinteri [17]; ■ – Levan–Royer [8]; □ – Couroneau–Royer [18]; ◆ – Shih–Chen [19]; △ – Shin–Cai (free-ends) [13]; ▼ – Shin–Cai (constrained-ends) [13].

Results and discussion. The geometrical evolution of the crack front, characterized as a part of an ellipse, was determined for each relative crack depth, *a*/*D*, through the crack aspect ratio, *a*/*b*. Fig. 3*a*, *b* shows how the crack grows in prestressing steel wires immersed in air and aggressive environment of $Ca(OH)_2$ + NaCl for different initial crack geometries: relative crack depth $(a/D)_i$ from 0.1 to 0.5; crack aspect ratio $(a/b)_i$ from 0.08 (quasi-straight crack front) to 1 (circular crack front).

Results show that fatigue crack propagation exhibits a preferential crack path towards which all *a*/*b*–*a*/*D* plots converge for the different initial crack geometries. This effect is quite quicker in air (higher exponent *m* of the Paris law) than in aggressive environment (with lower parameter *m* of the Paris law). If the initial crack front is quasi-straight, $(a/b)_i = 0.08$, fatigue crack propagation takes place with more curved fronts initially in air and later in aggressive environment (with the exception of initially deep cracks where *a*/*b* is always higher in air). On the other hand, starting from initially circular cracks, $(a/b)_i = 1$, fatigue crack propagation takes place with higher values of *a*/*b* (more curved fronts) in the case of aggressive environments.

Fig. 3*c*, *d* plots the evolution of maximum dimensionless SIF Y_{max} (the highest *Y*-value along the crack front) when the crack grows from different initial configurations in prestressing steel wires under conventional fatigue and corrosion-fatigue.

Generally, the value of the Y_{max} increases when so does the relative crack depth (*a*/*D*) and diminishes with the crack aspect ratio (*a*/*b*). In the fatigue crack growth the influence of the relative crack depth is higher than that of the aspect ratio, due to the existence of a preferential crack path (convergence in the plot *a*/*b*–*a*/*D*). Y_{max} is higher in the case of quasi-straight initial crack front, $(a/b)_i = 0.08$, than in the case of a circular one, $(a/b)_i = 1$. The situation is more pronounced when the crack propagation is small and when the initial cracks are deeper. In addition, Y_{max} exhibits an elevated convergence with the fatigue crack growth in all initial geometries of cracks analyzed in this paper, quicker in air than in the aggressive environment.

The ratio of minimum to maximum dimensionless SIFs Y_{min}/Y_{max} (Fig. 3*e*, *f*) tends to higher values for initially-straight crack fronts than in the case of initially-circular

crack fronts (although the trend is opposite for the initial stages of cracking). In addition, Y_{min}/Y_{max} is 1.0 (iso-K relationship) for all initial geometries when the crack reaches a relative depth of 0.8 in the case of fatigue in air but not in corrosion-fatigue.

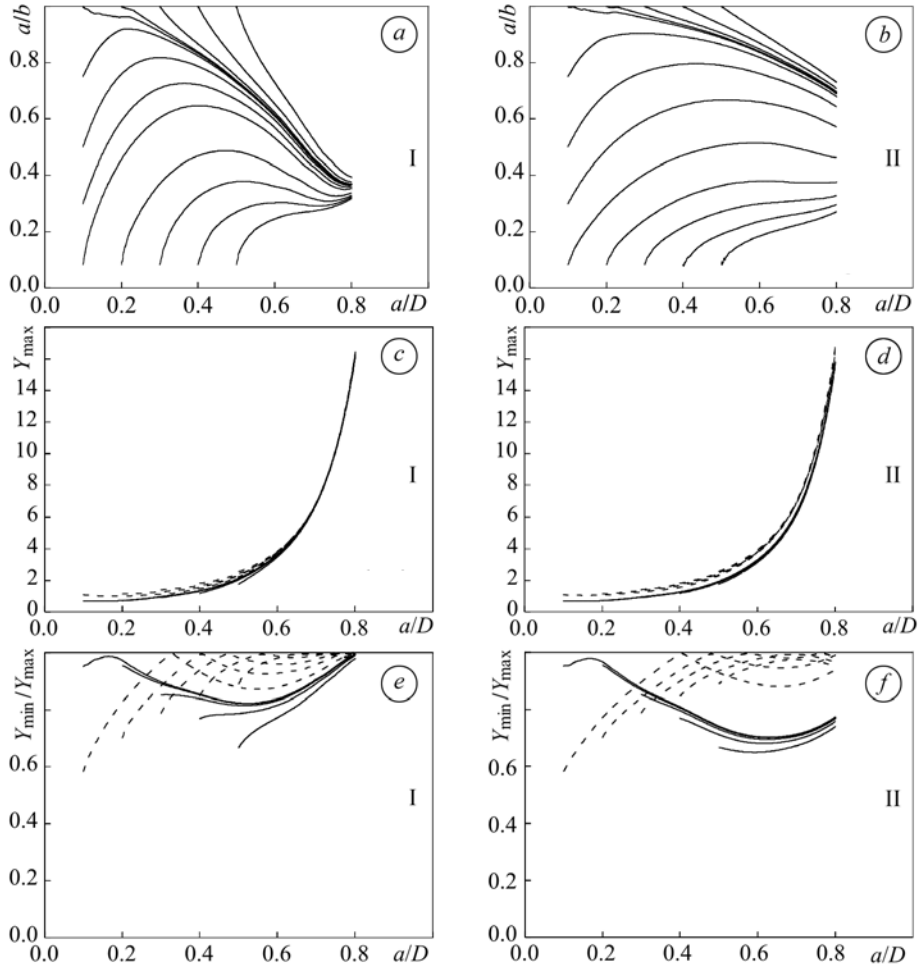

Fig. 3. Evolution of the crack aspect ratio (*a*, *b*), maximum dimensionless SIF (*c*, *d*) and Y_{min}/Y_{max} (*e*, *f*) in prestressing steel: fatigue in air (I) and $Ca(OH)_2$+NaCl corrosion– fatigue (II). (*c*, *d*, *e*, *f*) Dashed line – $(a/b)_i = 0.08$; solid line – $(a/b)_i = 1.0$.

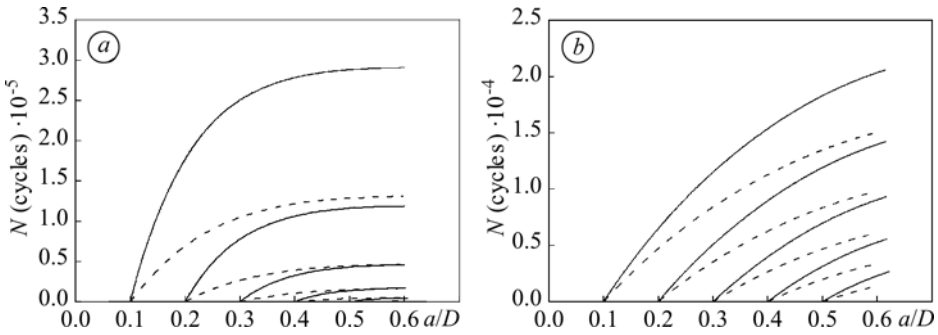

Fig. 4. Number of cycles necessary for fatigue crack propagation in prestressing steel: fatigue in air (*a*) and $Ca(OH)_2$ + NaCl corrosion– fatigue (*b*). Dashed line – $(a/b)_i = 0.08$; solid line – $(a/b)_i = 1.0$.

Fig. 4 shows the number of cycles necessary for fatigue crack propagation in air and aggressive environment (up to fracture following the local criterion $K_I = K_{IC}$) for $\Delta\sigma$ equal to $0.2\sigma_Y$ in the prestressing steel wire of 7 mm diameter. Fatigue life of initially straight cracks is shorter than the same of the initially circular cracks; therefore, caution should be taken in hydrogen assisted fracture processes in which the initial defect (hydrogen-assisted pre-damage) takes usually the form of a very shallow crack, whose geometrical model could tend to a quasi-straight flaw. In addition, it is observed how in corrosion-fatigue the number of cycles for fracture is lower, the plot being quasi-linear, while for the case of fatigue in air the number of cycles exhibits a pronounced slope change (very sloped at the beginning and quasi-horizontal at the end).

CONCLUSIONS

The following conclusions may be drawn on the basis of the numerical analysis performed in this paper:

(i) In all initial crack geometries analyzed in this paper, fatigue crack propagation in the prestressing steel exhibits a preferential crack path, where the convergence is quicker in air than in the solution of $Ca(OH)_2$ + NaCl, due the important decrease of the Paris exponent m in the case of aggressive environment.

(ii) If the initial crack front is quasi-straight, $(a/b)_i = 0.08$, fatigue crack propagation takes place with more curved fronts initially in air and latter in aggressive environment (with the exception of initially deeper cracks, where a/b is always higher in air). For initially circular cracks, $(a/b)_i = 1$, fatigue crack propagation takes place with higher values of a/b, i.e. more curved fronts, in the case of aggressive environment.

(iii) The dimensionless SIF (Y_{max}) exhibits, during fatigue crack propagation, a strong dependence on the relative crack depth and quite lower dependence on the crack aspect ratio (with the exception of shallow cracks of small depth), showing higher values for initially straight cracks than for circular ones. In addition, Y_{max} exhibits a quicker convergence during fatigue crack growth, higher in air than in the aggressive environment.

(iv) Fatigue life of initially circular cracks is longer than the same in initially quasi-straight cracks (therefore, caution should be taken in hydrogen assisted fracture processes). In addition, it is observed how in corrosion-fatigue the deleterious effect of the aggressive environment on material performance consists of a clear decrease of the corrosion-fatigue life in relation to the service life under cyclic loading in air.

РЕЗЮМЕ. Описано еволюцію фронту поверхневої тріщини в сталевих дротах для переднапруженого стану залізобетону, підданих втомному навантаженню на повітрі і корозійній втомі в середовищі $Ca(OH)_2$ + NaCl. На основі дискретизації чисельно змодельовано фронт тріщини, який приймали еліптичним, і вважали, що тріщина в кожній точці просувається перпендикулярно до її фронту згідно з законом Періса–Ердогана. Використовували трипараметричний розв'язок для коефіцієнта інтенсивності напружень (КІН). Кожний з аналізованих випадків, якому відповідала певна початкова геометрія тріщини, характеризувався еволюцією форми напівеліптичної тріщини (відношення півосей еліпса) і відносної її глибини, а також варіацією значень максимального безрозмірного КІН вздовж фронту тріщини.

РЕЗЮМЕ. Описана эволюция фронта поверхностной трещины в стальных проволоках для преднапряженного состояния железобетона, подвергаемых усталости на воздухе и коррозионной усталости в среде $Ca(OH)_2$ + NaCl. На основе дискретизации численно смоделирован фронт трещины, который принимали полуэллиптическим, и считали, что трещина в каждой точке движется перпендикулярно к ее фронту согласно закону Пэриса–Эрдогана. Использовали трехпараметрическое решение для коэффициента интенсивности напряжений (КИН). Каждый из анализированных случаев, которому соответствовала определенная начальная геометрия трещины, характеризовался эволюцией формы полу-

эллиптической трещины (отношение полуосей эллипса) и относительной ее глубины, а также изменением значений максимального безразмерного КИН вдоль фронта трещины.

Acknowledgements. The authors wish to acknowledge the financial support provided by the following Spanish Institutions: Ministry for Science and Technology (MCYT; Grant MAT2002-01831), Ministry for Education and Science (MEC; Grant BIA2005-08965), Ministry for Science and Innovation (MICINN; Grant BIA2008-06810), Junta de Castilla y León (JCyL; Grants SA067A05, SA111A07 and SA039A08).

1. *Toribio J., Matos J. C., and González B.* Micro- and macro-approach to the fatigue crack growth in progressively drawn pearlitic steels at different R-ratios // Int. J. Fatigue. – 2009. – **31**. – P. 2014–2021.
2. *Toribio J. and Kharin V.* Role of crack tip mechanics in stress corrosion cracking of high-strength steels // Ibid. – 2004. – **126**. – P. L57–L63.
3. *Murtaza G. and Akid R.* Empirical corrosion fatigue life prediction models of a high strength steel // Engng. Fract. Mech. – 2000. – **67**. – P. 461–474.
4. *Martín A. and Sánchez-Gálvez V.* Environmentally assisted fatigue crack growth in high strength eutectoid cold drawn steel // Br. Corros. J. – 1988. – **23**. – P. 96–101.
5. *Singh N. and Sánchez-Gálvez V.* Effect of $Ca(OH)_2$+ NaCl environment corrosion fatigue crack growth in cold drawn eutectoid steel rods // Ibid. – 1991. – **26**, – P. 117–121.
6. State-of-the-art of corrosion testing by using electrochemical noise measurements / J. Goellner, A. Burkert, A. Heyn, E. Boese, O. Ezers'ka, and J. Hickling // Mater. Sci. – 2001. – **37**. – P. 509–519.
7. *An automated* procedure for the geometrical modelling of a surface crack front / J. Toribio, J. C. Matos, B. González, and J. Escuadra // Struct. Durab. Health Monit. – 2009. – **123**. – P. 1–16.
8. *Levan A. and Royer J.* Part-circular surface cracks in round bars under tension, bending and twisting // Int. J. Fract. – 1993. – **61**. – P. 71–99.
9. *Paris P. C. and Erdogan F.* A critical analysis of crack propagation laws // J. Basic Eng. – 1963. – **85D**. – P. 528–534.
10. *Carpinteri A.* Shape change of surface cracks in round bars under cyclic axial loading // Int. J. Fatigue. – 1993. – **15**. – P. 21–26.
11. *Numerical* modelling of crack shape evolution for surface flaws in round bars under tensile loading / J. Toribio, J. C. Matos, B. González, and J. Escuadra // Engng. Fail. Anal. – 2009. – **16**. – P. 618–630.
12. *Lin X. B. and Smith R.* A. Shape growth simulation of surface cracks in tension fatigued round bars // Int. J. Fatigue. – 1997. – **19**. – P. 461–469.
13. *Shin C. S. and Cai C. Q.* Experimental and finite element analyses on stress intensity factors of an elliptical surface crack in a circular shaft under tension and bending // Int. J. Fract. – 2004. – **129**. – P. 239–264.
14. *A critical* review of stress intensity factor solutions for surface cracks in round bars subjected to tension loading / J. Toribio, N. Álvarez, B. González, and J. C. Matos // Engng. Fail. Anal. – 2009. – **16**. – P. 794–809.
15. *Valiente A.* Criterios de fractura para alambres // PhD thesis. – Spain: Polytechnic University of Madrid, 1980.
16. *Astiz M. A.* An incompatible singular elastic element for two- and three-dimensional crack problems // Int. J. Fracture. – 1986. – **31**. – P. 105–124.
17. *Carpinteri A.* Elliptical-arc surface cracks in round bars // Fatigue Fract. Engng. Mater. Struct. – 1992. – **15**. – P. 1141–1153.
18. *Couroneau N. and Royer J.* Simplified model for the fatigue growth analysis of surface cracks in round bars under mode I // Int. J. Fatigue. –1998. – **20**. – P. 711–718.
19. *Shih Y.-S. and Chen J.-J.* The stress intensity factor study of an elliptical cracked shaft // Nucl. Engng. Des. – 2002. – **214**. – P. 137–145.

Received 11.02.2011